Experimental and numerical investigations of dual gauge railway track behaviour

Ignacio Villalba Sanchis *, Ricardo Insa Franco, Pablo Martínez Fernández, Pablo Salvador Zuriaga

Dept. of Transport Infrastructure and Engineering, Universitat Politècnica de València (UPV), Spain

HIGHLIGHTS

- A comprehensive experimental campaign in dual gauge track in Spain.
- Vibration experiments with train passage validating a three-dimensional FEM.
- Novel insights into the contact pressure of the dual gauge sleepers are highlighted.
- The unsymmetrical response of the dual gauge track should be considered to make decision on the design and maintenance of dual gauge tracks.

ARTICLE INFO

ABSTRACT

The dual gauge track, in which a third rail is added to the conventional track section, has recently been installed in large sections of the Spanish railway network, allowing the passage of trains of two different track gauges. With increasing train speeds and axle loads, the new dual gauge track must share the main characteristics of current track systems while minimizing the drawbacks, in order to ensure a real step forward in railway track design. Thus, this paper presents a research study on the dynamic behaviour of a dual gauge track generated by the passage of trains. To accomplish this task, an extensive experimental and numerical investigation was conducted in a stretch of the Spanish railway network. The experimental work includes the characterization of the rail and sleeper mechanical behaviour during train passage. In addition, results from the experimental investigations were also compared with a fully three-dimensional numerical model. The model uses SOLID95 elements with elastoplastic Mohr–Coulomb behaviour and yields a rMSE of 25% between measured and calculated responses, hence showing a good agreement. Concerning the vibrational response, the presence of the third rail have a significant effect, since the maximum rail vertical accelerations significantly increased on the side where two rails are close together. Finally, the contact pressure between the sleeper and the ballast bed is 35% higher in the common rail when the train runs on the Iberian gauge, but 50% higher on the dedicated rail when the train runs on the standard gauge.

1. Introduction

The traditional track gauge in the Spanish railway network is the Iberian track gauge, established in the 19th century and equal to 1668 mm. However, the most widespread track gauge in the rest of Europe is the standard gauge, which is equal to 1435 mm, thus creating a break of gauge in Spain that adds delays, cost, and inconvenience.

Moreover, after considering various strategies, in 1988 the Spanish government decided to design and build all new high-speed lines with the standard gauge, connecting these new rail lines with the rest of Europe. After huge investments in the latest decades, the current Spanish high-speed system is the longest one in Europe with more than 3200 km and the second longest in the world after China.

Since the development of Spanish high-speed railway lines, the coexistence of two different track gauges has been a problem for operators and passengers alike, creating frontiers among high-speed and conventional lines. To solve interoperability issues and ensure that trains may use both rail lines and connect with the rest of Europe, a few specific solutions have been tested and implemented in Spain. Traditionally, passenger and freight were transhipped between trains with different gauges, mostly in the border between Spain and France, with the logical delay and

* Corresponding author at: Camino de Vera, s/n, Building 4A, 1st Floor, 46022 Valencia, Spain.
E-mail address: igvilsan@cam.upv.es (I. Villalba Sanchis).

I. Villalba Sanchis, R. Insa Franco, P. Martínez Fernández et al.

Construction and Building Materials 299 (2021) 123943

increased costs that this operation entails. Alternatively, train gauges could be modified by lifting up the trains and replacing wheelsets or bogies, a solution more comfortable for passengers but still time-consuming.

To address this issue, in the case of passenger trains, special wheelset systems (known as Variable Gauge Axle, VGA; or, alternatively, Gauge Adjustable Wheelsets, GAW) have been highly developed since the late 60s, which allow trains equipped with them to operate on both Iberian and standard-gauge lines. This kind of solution also requires the installation of gauge changers to manage the transition between lines with different gauges. On the other hand, GAW systems for freight trains are still far from being fully developed and implemented, as higher axle loads complicate the design and operation of such systems.

However, both trains and facilities must be designed, installed, and maintained under adequate conditions, all of which raises costs and hinders their development. In addition, important problems continue to exist with regard to freight trains, since automatic track gauge changeover has not been successfully designed for them.

To solve these problems a special track solution has been recently implemented in different stretches of the Spanish railway network, consisting on a three-rail track with dual gauge (Fig. 1). This solution is expected to decrease the negative impacts associated with road traffic and to have positive impacts on the environment thanks to the modal transfer to rail. Although there are a few dual gauge tracks in other railways around the world, these solutions are restricted to harbour or yard areas, where the speed is usually lower than 30 km/h. In contrast, the new dual gauge track system is conceived for speeds up to 200 km/h. This allows a considerable reduction of costs compared to using separate tracks but introduces several technical complexities and challenges in track design, operation and maintenance, because of the large number of suburban, regional and high-speed trains running on the network.

Thus, the dual gauge track system means a substantial modification of the conventional track and requires an adequate and accurate analysis, especially in terms of ground borne vibrations, which also aids in the implementation of suitable vibration mitigation measures. This issue may be approached both numerically and experimentally. In the first case, numerical simulations are useful tools for evaluating the vibration behaviour of the rail vehicle and track elements where input parameters are well defined. In this field, the finite element method (FEM) [1–4], the boundary element method (BEM) [5,6] and the combined FEM-BEM [8,8] were mostly used to determine the vibrational response of railway track due to the passage of trains. A drawback of these theoretical approaches is that several assumptions must be made concerning train characteristics, track properties and boundary conditions.

Meanwhile, in the case of dual gauge tracks, the uncertainty caused by the addition of the third rail adds further complexity to previous numerical models. Furthermore, in case of mixed corridors, the demands for track smoothness and load carrying capacity become a major concern. Under this scenario, the principal advantage of an experimental study over a numerical one is that a reduced number of modelling assumptions are required. Therefore, physical testing is the most appropriate method to obtain the response of railway track [3,4,9,10]. Despite this, there is no published literature related to the experimental analysis of vibration from dual gauge tracks due to the specific design of this superstructure. Therefore, it is not clear what the ground vibration characteristic and propagation are when the train runs along a specific gauge. It is also unknown whether the existing theoretical models can still be applicable to predict train induced ground vibrations. As a result, lack of experience of maintenance and lack of standards for the design are also important disadvantages.

Thus, this paper attempts to introduce the most recent experiment accomplished by the authors on dual gauge track, which contribute to a deeper understanding of this special track. Accordingly, measurements were taken in both Iberian and standard gauge and analysed in the time domain to gain a comprehensive understanding of behaviour of the complicate dual gauge track design. The presented model represents a very significant contribution to the existing panorama in terms of computational tools for dual gauge railway track analyses. The consideration of the soil or natural ground response were outside this scope because they are strongly influenced by the nature of the materials as well as site conditions, which may even change significantly along the railway line.

The paper is structured as follows: First, a description of the experimental study is given, with detailed explanation of the sensors installed on the track and the data gathering. Secondly, the numerical FEM model is described, including its main features and parameters. Afterwards, both the experimental and numerical results are analysed and compared in order to characterise the dynamic behaviour of the dual gauge track. Finally, the main conclusions reached are exposed.

2. Experimental study

The experimental evaluation of the vibrations and displacements induced by railway traffic is a fundamental step for further investigations and validation of prediction models. Accordingly, in June 2019 a field measurement on the Valencia-Castellón dual gauge railway track was performed. This line is part of the Mediterranean Corridor, which is operated with different train services whose speeds range between 80 and 160 km/h. Monitored slow trains (commuters and freight) ran on Iberian gauge while high-

Fig. 1. Conventional railway track (right) and dual gauge track (left) in Spain.

I. Villalba Sanchis, R. Insa Franco, P. Martínez Fernández et al.

Construction and Building Materials 299 (2021) 123943

speed trains ran on standard gauge. The measurement site is placed near Massalfasar station, located 15 km north of Valencia (Fig. 2).

2.1. Track structure

The test section is a double-line railway with low embankment. The track is a typical ballast track composed of ballast, subballast and sub-grade layers, with thicknesses 0.3, 0.3 and 1.5 m, respectively. The three rails are continuously welded UIC 60 rails, with a mass per unit length of 60 kg/m, fixed to newly designed third-rail, 400 kg prestressed concrete sleepers AM-05 via Vossloh clips, spaced 0.6 m. Ballast is siliceous, with an average stone size 31.5 and 50.0 mm. Each singular ballast element has a polyhedral shape, and its largest dimension must be less than three times its shortest dimension, according to the shape index test (Fig. 3).

2.2. Test scheme

In order to obtain the dynamical response of the dual gauge track, two distinct test setups were deployed. The first one records different component vibration levels at rail and sleeper, while the second records vertical displacements between rail and sleeper and between rail and ballast. Accelerometers were held in place vertically by gluing them onto the surfaces, while distance meters were fixed to the rail and sleeper by using powerful magnets (Fig. 4). The acceleration sensors were carefully selected according to the location of the measuring points. All sensors were connected to (and powered by) an acquisition system placed near the track, which in turn was connected to a laptop for data storage.

Specifically, the first setup consisted of five accelerometers whose characteristics and specific location in the track are detailed in Table 1. The accelerometers were connected to a four-channel signal conditioner, which in turn was connected to the laptop.

For the second setup, two potentiometers were used, both with a range up to 100 mm and a sensibility of 1.19 V/cm. As Fig. 4 shows, one potentiometer was placed to measure relative displacements between rail and sleeper, and the other to measure relative displacements between rail and ballast. These sensors were also linked to a data acquisition instrument system to detect the dynamic responses of the track components. In all cases, measurements were performed on straight parts of the track for each train passing (Fig. 5).

Finally, the sampling frequency was set to 4000 Hz for all measurements. In the data processing, background vibration noise and other possible interferences were removed by using a 4-order band-pass digital Butterworth filter with a 1000 Hz cut-off frequency. Due to one-side access allowed by the Administrator of Railway Infrastructures (ADIF) at the test track site, the measuring unit was installed on the outside of the dual gauge track.

With all of this equipment, a large dataset was obtained comprising the passage of several distinct trains running at different speeds. The data measured during one of the passages of the high-speed and commuter trains was employed in the experimental validation of the developed numerical model.

2.3. Train characteristics

Due to its proximity to the city of Valencia, the studied site has a very significant traffic volume. From the range of trains circulating in the studied railway track, the following types may be highlighted: a high-speed train (Ave Class 100) and a commuter train (Civia). On one hand, the selection of these trains is justified by their gauge, considering that each type of train runs on a specific gauge (1435 mm for high-speed and 1668 mm for commuter trains). On the other hand, it can be explained by the existence of plenty available information about the commuter and high-speed trains.
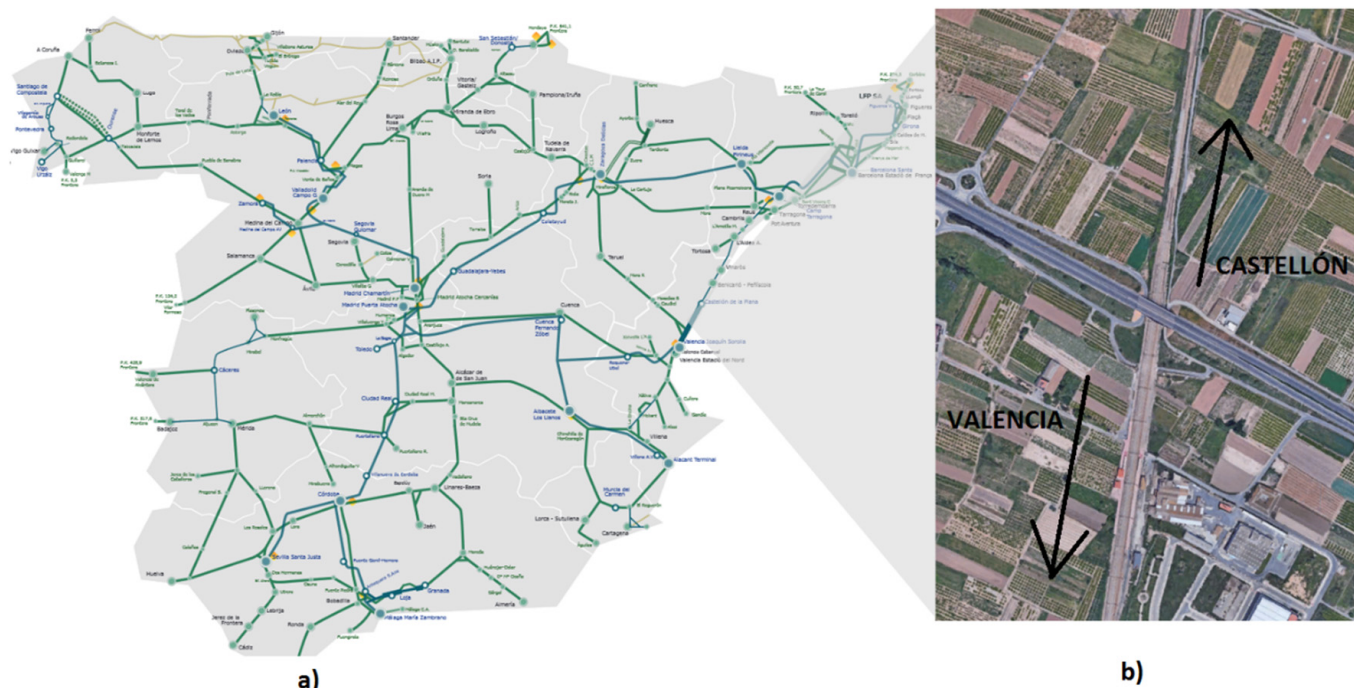

Fig. 2. General view (a) and detailed location (b) of the test track site.

I. Villalba Sanchis, R. Insa Franco, P. Martínez Fernández et al.

Construction and Building Materials 299 (2021) 123943

Fig. 3. View of dual gauge railway track (a) and detail of rail fasteners at the double rail side (b).
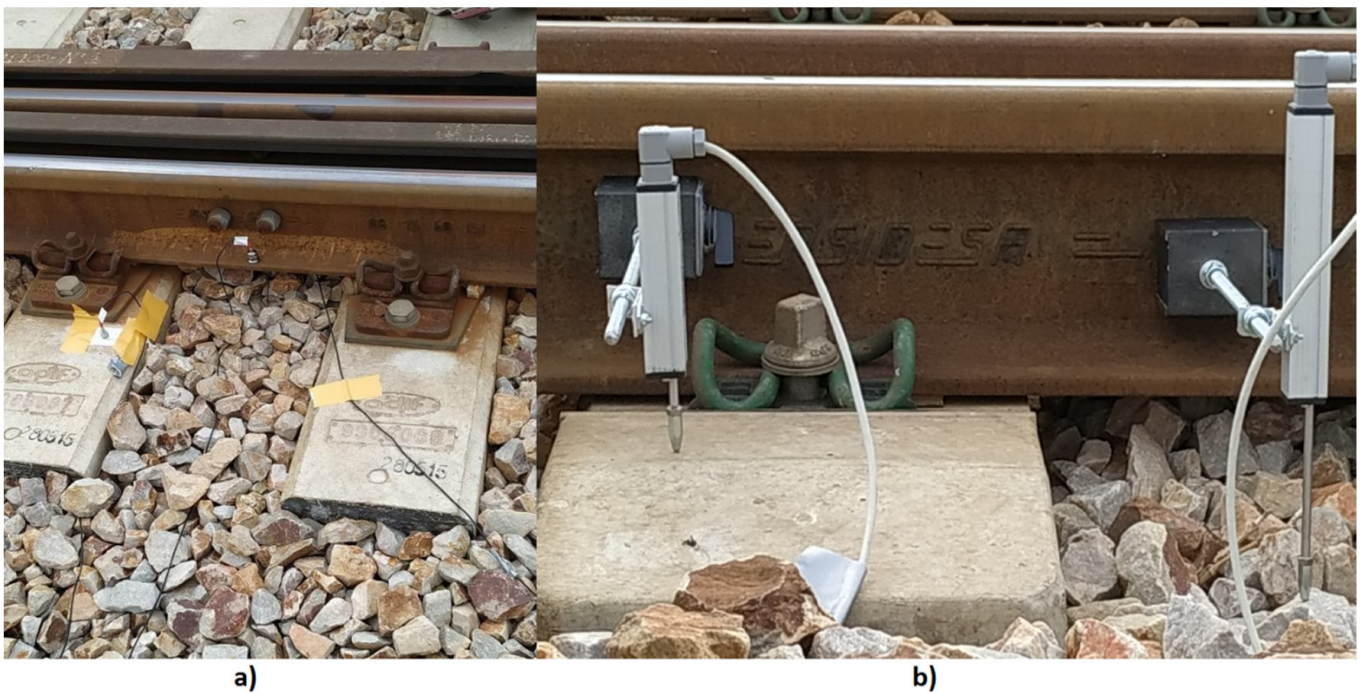

Fig. 4. Accelerometers (a) and distance potentiometers (b).

Table 1
Characteristics of accelerometers.

Sensor range (g)	Sensitivity (mV/g)	Location
±600		Rail foot (common rail)
	10	
±600	10	Rail foot (inner rail)
±600	10	Rail foot (outer rail)
±55	100	Sleeper
±5	1000	Ballast

A brief description of each train follows, with their principal characteristics.

2.3.1. High-speed train (Ave Class 100)

The S-100 high-speed train is manufactured by Alstom and started commercial operation in 1992. The trainsets are designed for high-speed services on standard gauge, with two motorized bogies each and eight passenger cars with shared bogies. Its total length is 200 m. During the experiment, the axle load was around 12 t for passengers' coaches and 18 t for traction units, according to
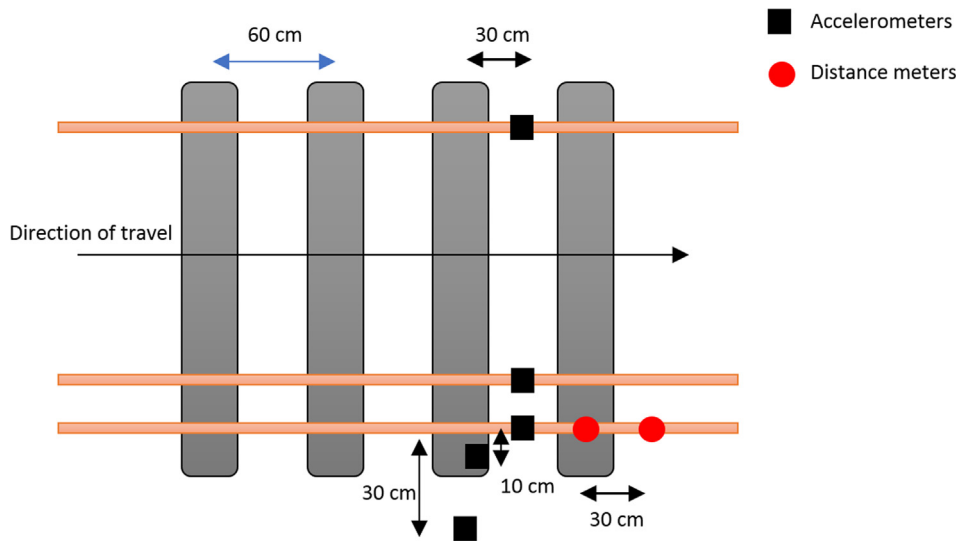
I. Villalba Sanchis, R. Insa Franco, P. Martínez Fernández et al.

Construction and Building Materials 299 (2021) 123943

Fig. 5. Schematic diagram of measuring points.

RENFE train characteristics [11]. Table 2 shows the specifications of the AVE Class 100 trainset.

2.3.2. Commuter train (Civia)

Civia series train were developed in 2000 by CAF and Siemens, covering the major metropolitan areas in Spain. Civia trains are modular and may comprise two, three, four or five cars with cabins at both ends. In this case, the monitored Civia trains consist of four cars with a total length of 80 m and an axle load of 13 t [11], running on Iberian gauge. Table 2 shows the specifications of the Civia trainset.

3. FE model for the analysis of the dual gauge track response

3.1. Overview

The reproduction of the railway track response under train loads in terms of displacements, accelerations and stresses can be predicted using a wide variety of models, from half-track analytical models up to complex numerical models. However, the versatility of the latter allows over-coming some of the limitations of the analytical and semi-analytical approaches.

In the latest years, different numerical models defining the track response due to train loads have been developed and tried [6,7,10,12–17]. According to previous studies, numerical models has been successfully applied to simulate the dynamic response of railway tracks. Specifically, FEM allows for the construction of large track models which provides a non-linear solution and a three-dimensional stress state of different railway track components. In addition, the track may often be assumed as a symmetrical structure. However, none of these studies takes into consideration the presence of the third rail, which represents the distinctive feature of the dual gauge track. In this case, it is not possible to study the behaviour of the entire system by considering

only one of its halves. Accordingly, the total response can be only obtained by modelling the entire track section. To accomplish this task, this paper presents a 3D numerical model that allows the calculation of track settlements and vibrational response, explicitly considering the presence of a third rail.

3.2. Modelling the structure

Because the behaviour of the dual gauge track involves three-dimensional phenomena that are not considered when the model is simplified to two dimensions, a three-dimensional modelling process is considered. The model consists of the application of a FEM for dual gauge track by explicitly considering the presence of a third rail. To accomplish this task a commercial software ANSYS® Mechanical APDL 17.2 was used. In the analysis of problems involving displacements or vibrations induced by railway traffic, the track may often be assumed as a symmetrical. Nevertheless, the unusual asymmetry of the track due to the presence of the third rail requires a new model that takes this feature into account.

Table 2
Characteristics of trains.

Parameters	High-speed train	Commuter train
Maximum axle weight (t)	Tra. unit: 18 / Pas. car: 12	13
Length (m)	185	80
Train speed at test site (km/h)	150-160	80-90
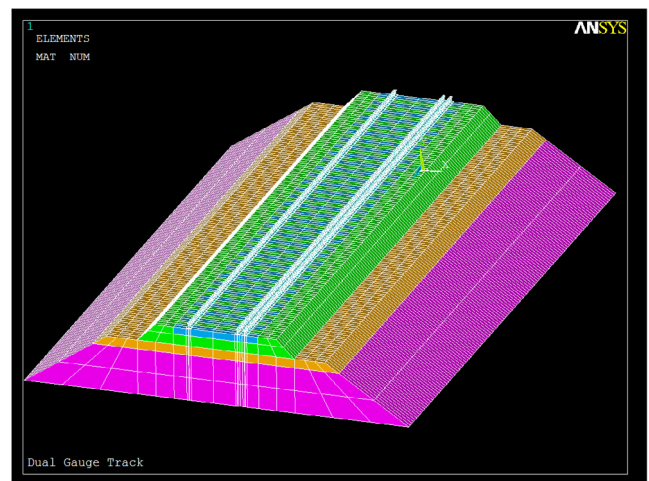
Fig. 6. View of case-study homogeneous model, 33 sleepers long, showing finite element mesh.

I. Villalba Sanchis, R. Insa Franco, P. Martínez Fernández et al.

Construction and Building Materials 299 (2021) 123943

Table 3
Material parameters considered in the finite element analysis.

Materials	Young modulus (MPa)	Poisson's ration	Density (kg/m^3)
Rail	210,000	0.30	7860
Sleeper	30,000	0.25	2350
Ballast	130	0.20	1730
Subballast	300	0.30	2200
Embankment soil	100	0.40	2050

The elements employed for the model must change between different elements. For railway steel I section, SOLID95 was selected, which is defined by 20 nodes and three degrees of freedom at each node (translations in the nodal x, y, and z directions). The SOLID65 and Link180 elements were used to model concrete and steel sleepers, taking into account the UIC60 rail profile and a pre-stressed concrete monoblock AM-05 (assuming rectangular prisms with 2.75 m length, 0.30 m width, 0.23 m height and 400 kg each). Rails were joined to the sleepers by fastenings characterized by a set of linear spring elements in vertical, lateral and longitudinal directions. In addition, the rotational stiffness between the rail and the sleeper provided by the fasteners was simulated by an elastic rotational spring in the vertical direction. The substructure was composed of granite ballast and sub-ballast

layers, 0.3 m thick each, modelled using SOLID95 elements with elastoplastic Mohr–Coulomb behaviour. The embankment was assumed to be a homogeneous, isotropic, well-compacted and reasonably stiff soil, with 3 m thickness. The boundary conditions imposed on the planes that limit the model are restrictions that prevent perpendicular movement at these planes. By means of this model, the track superstructure and substructure can be analysed as a whole, providing a global vision of the track behaviour when subjected to specific train loads.

As per the model size, 33 sleepers were considered along the rail at 0.6 m interval spacing. The geometric dimensions are thus 20, 12.5 and 4 m in the longitudinal, horizontal and vertical directions, respectively. This ensures that the model is big enough to allow a wave to travel but not to reflect in the boundaries, a circumstance which may degrade the accuracy of the overall solution. In this way, the finite element model acquires the form shown in Fig. 6, to facilitate the understanding of its longitudinal development.

The properties of all materials are summarized in Table 3. These values are based on the recommendations provided in current normative [18], considering the particular geometry and the elements that form the section of dual gauge railway track installed in Spain.

Finally, the dynamic simulations were performed considering the passing of single bogies or axles belonging to two railway vehicles as described previously (Section 2.3). Accordingly, the vehicle
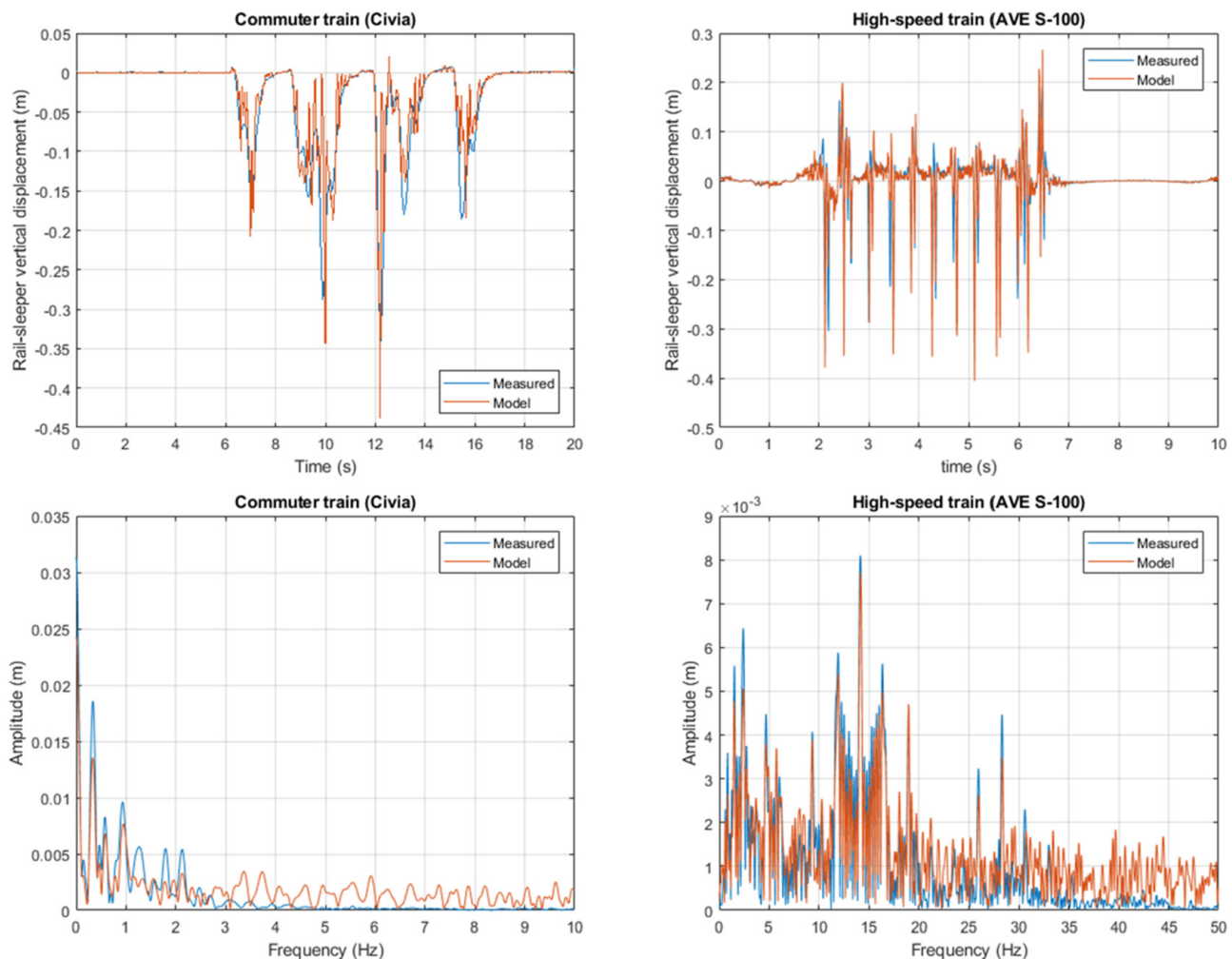

Fig. 7. Vertical displacement and frequency spectra between the rail-sleeper during train passages.

I. Villalba Sanchis, R. Insa Franco, P. Martínez Fernández et al.

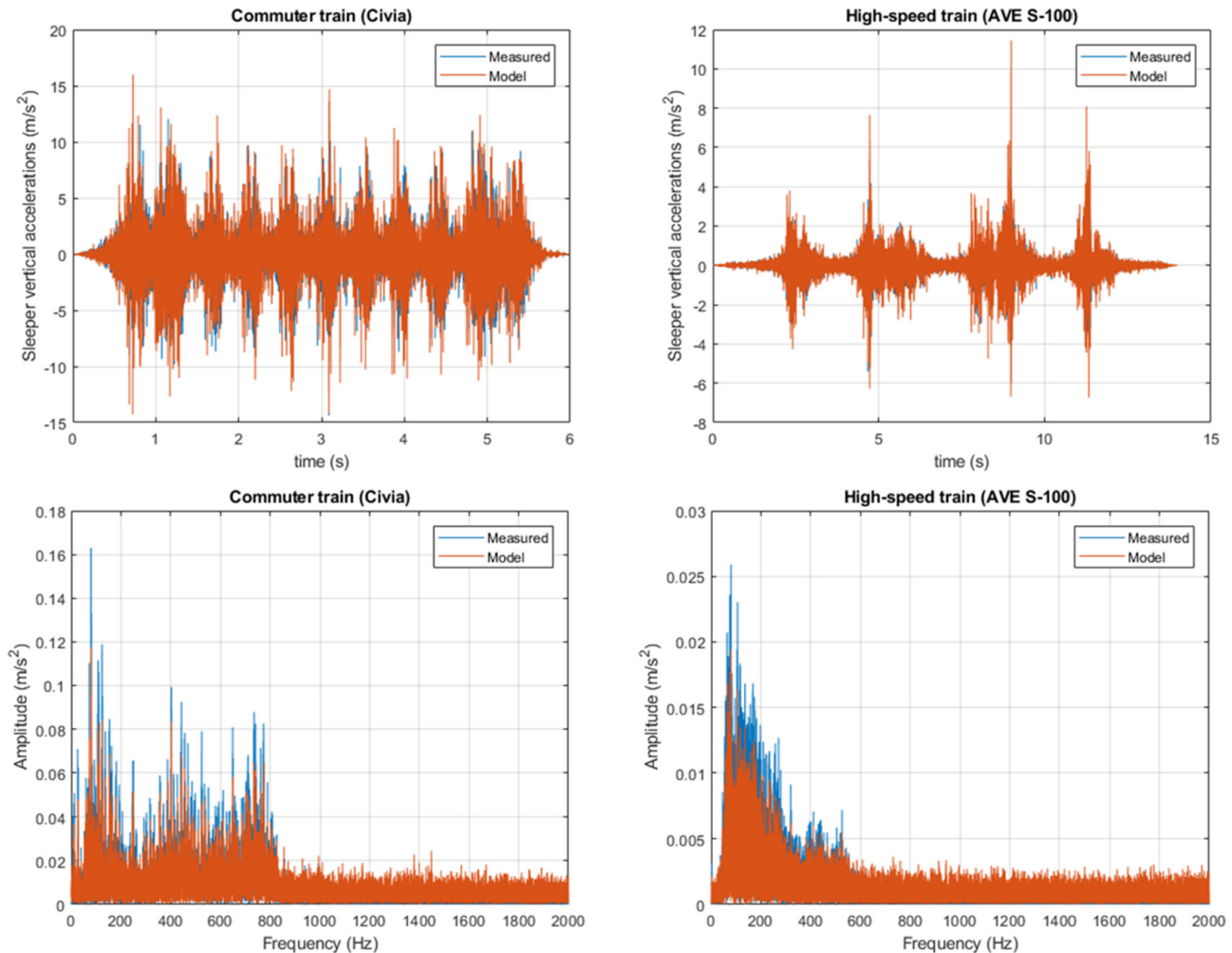Construction and Building Materials 299 (2021) 123943

Fig. 8. Vertical accelerations and frequency spectra on the sleeper during train passages.

model is simplified as a single/double row concentrated moving load.

3.3. Model validation with field measurements

In order to validate the proposed model, comparisons between measured and calculated track responses during the passage of several trains were performed. Train loads are modelled as moving point loads. Each time increment $\triangle t$, loads are displaced a distance equal $V\triangle t$, being V the train speed, and applied to the nearest nodes inversely proportional to the distance. In this way, the model dynamic response at a given node i is the sum of the responses at this node produced by the moving load applied subsequently to each node j. The model is computed for a single bogie and the overall train response is obtained by shifting and scaling the axle load of subsequent bogies. The goodness of fit is evaluated by computing the relative mean squared error (rMSE), given by Eq. (1)

$$rMSE = \frac{\frac{\sum_{i=1}^{n}\left(\widehat{x}_i - x_i\right)^2}{n}}{\mathrm{var}(\mathbf{x})} \qquad (4)$$

where $\widehat{x}$ is the data vector of values given by the model, $\mathbf{x}$ is the data vector of registered values and var($\mathbf{x}$) is its variance. Both vectors have n elements. According to [21], a model behaves correctly if the rMSE falls below 20% of data variance. Starting with the analysis of the track response, Fig. 7 presents the comparison between the

computed vertical displacement between the rail-sleeper interface and the measurement given by the distance meter system. Therefore, these graphics superpose measured and modelled vertical displacements (expressed in time-scale and also as frequency spectra).

The comparison shows a fair agreement between the numerical and the experimental results for the commuter train (rMSE = 35%), and better results for the high-speed train (rMSE = 26%). In fact, the ability showed by the numerical model is remarkable. For the commuter train, only the first carriage is well represented by the model. Discrepancies in the second and third carriages are mainly due to the uncertainty in the actual axle loads. In terms of frequency content, the model correctly reproduces frequencies below 1 Hz. Frequencies between 1 and 3 Hz show higher discrepancies, whereas frequencies beyond 3 Hz have no significant influence. For high-speed train, it is seen that uplift movement develops in the rail fasteners before the arriving of the train axles, albeit with limited amplitude (around 0.2 mm). Thus, small differences may again be explained due to the complexity of the interaction between vehicle and track, as well as the existence of wheel or rail defects. In terms of frequency, the model correctly reproduces the most relevant frequencies in the 0–30 Hz band.

Concerning the sleeper response, Fig. 8 compares experimental and numerical accelerograms and frequency spectra of the vertical acceleration of the sleeper induced by the passage of commuter and high-speed trains. Results yield rMSE values for commuter and high-speed trains of 25.7% and 26.4%, similar and close to
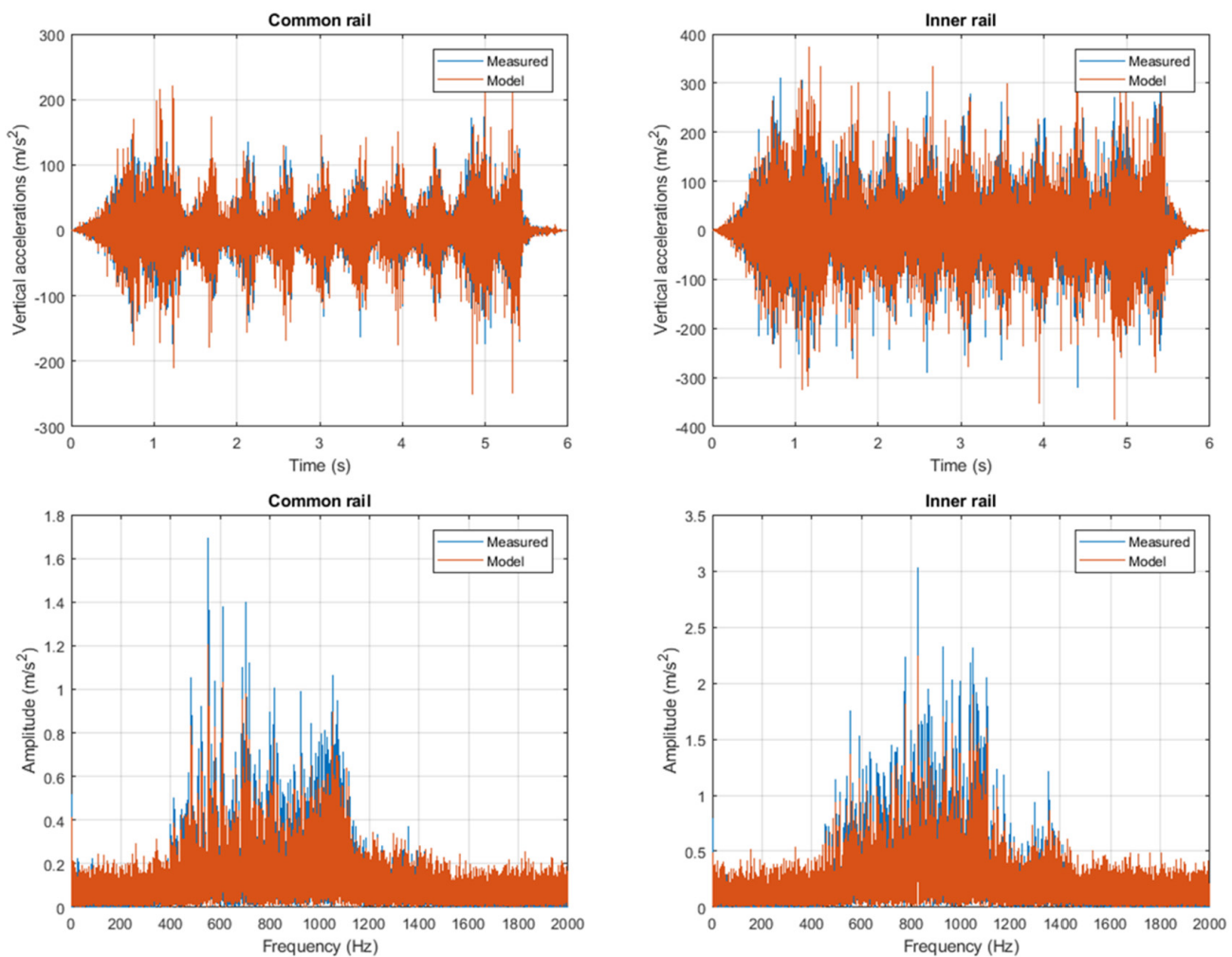
Fig. 9. Time-histories comparison of rail vertical vibration accelerations and frequency spectra, AVE Class 110 train.

the threshold of 20%. By observing these results, the model was able to provide a good agreement in terms of timing, magnitude and shape of the sleeper vertical accelerations. In terms of frequency, the model also correctly shapes the most important frequencies detected in the measurements.

Given the results shown above, the numerical model leads to a very reasonable assessment of the main aspects of the dual gauge track superstructure. It should be noted that the agreement between the calculated and the measured results corresponds to a partial validation of the developed numerical model. This is because the present work focuses on the mechanical phenomena occurring on the rail-sleeper grid of the dual gauge track. The model does not consider wheel-rail interaction forces since there was no possibility to measure them during the data gathering.

4. Dual gauge track response

As emphasized above, the main objective of the study is to identify the dynamic behaviour of a dual gauge track generated by the passage of trains. Since the track described previously was in operation, trains were circulating at different speeds that may be considered as representative of a real traffic scenario. Therefore, numerous tests were carried out by measuring acceleration and displacement signals in various track positions, considering speeds

from 80 to 90 km/h for Civia trains and from 150 to 160 km/h for AVE Class 100 trains.

4.1. Characteristic of vibration on dual gauge track

As mentioned before, several train passages were recorded during the experimental campaign. Vibrations were analysed in terms of accelerations as a function of time. Fig. 9 shows the accelerogram and frequency spectra of the rail vertical accelerations during the passage of the AVE Class 100 at 150 km/h, running on the standard gauge. To analyse whether there is a difference between rails, it was thought appropriate to analyse the response of each rail separately, considering the gauge in which each train is running. As can be seen, each train bogie induced a cluster of significant vertical rail vibration values.

The model adjustment yields an rMSE of 24.9% for the common rail and 25.2% for the inner rail. As can be seen, higher amplitudes of vibrations were generated on the inner rail, which corresponds to the standard gauge. Particularly, the maximum amplitude of vertical accelerations was approximately 300 m/s^2, while the common rail reaches peak values around 200 m/s^2. In terms of frequency, the common rail shows the greatest amplitudes at frequencies around 600 Hz, whereas the inner rail shows its max-
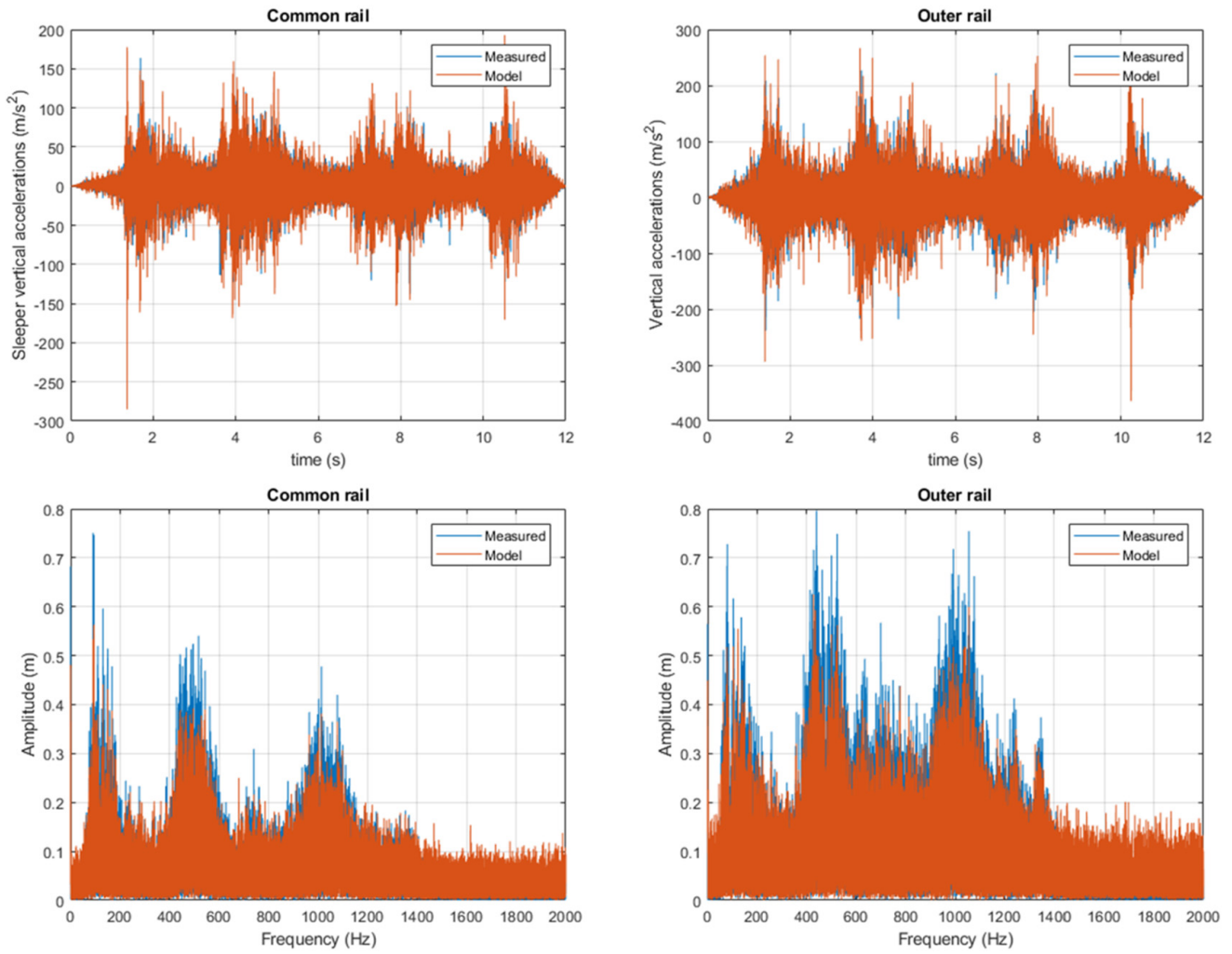
Fig. 10. Time-histories comparison of rail vertical vibration accelerations and frequency spectra, Civia train.
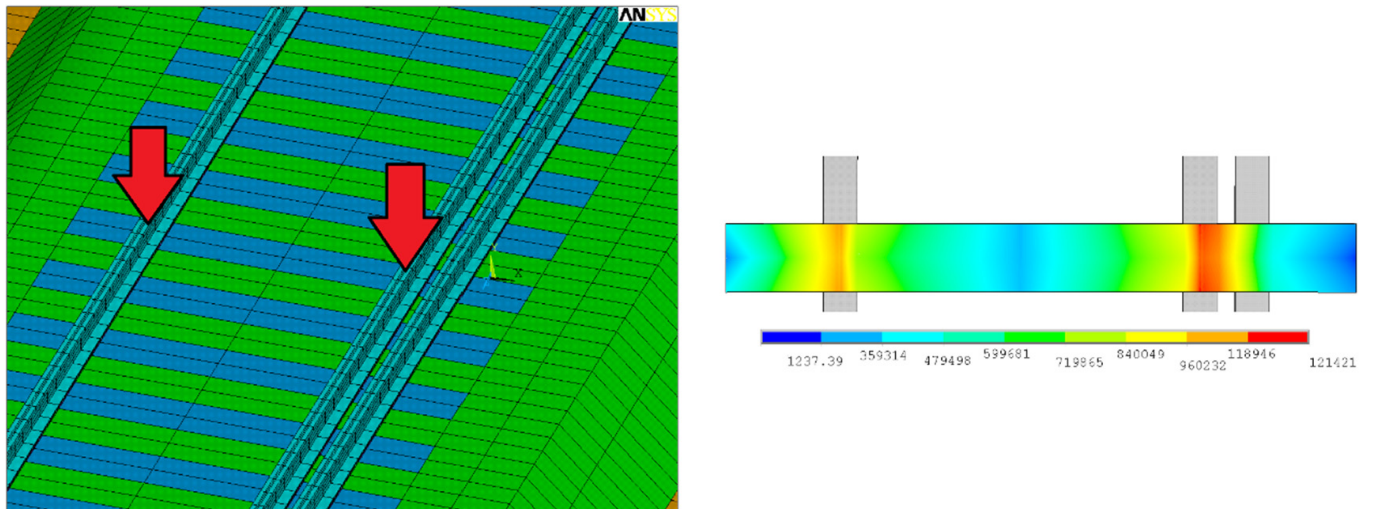

Fig. 11. Contact force distribution on sleeper-ballast interface, AVE Class 100 train.
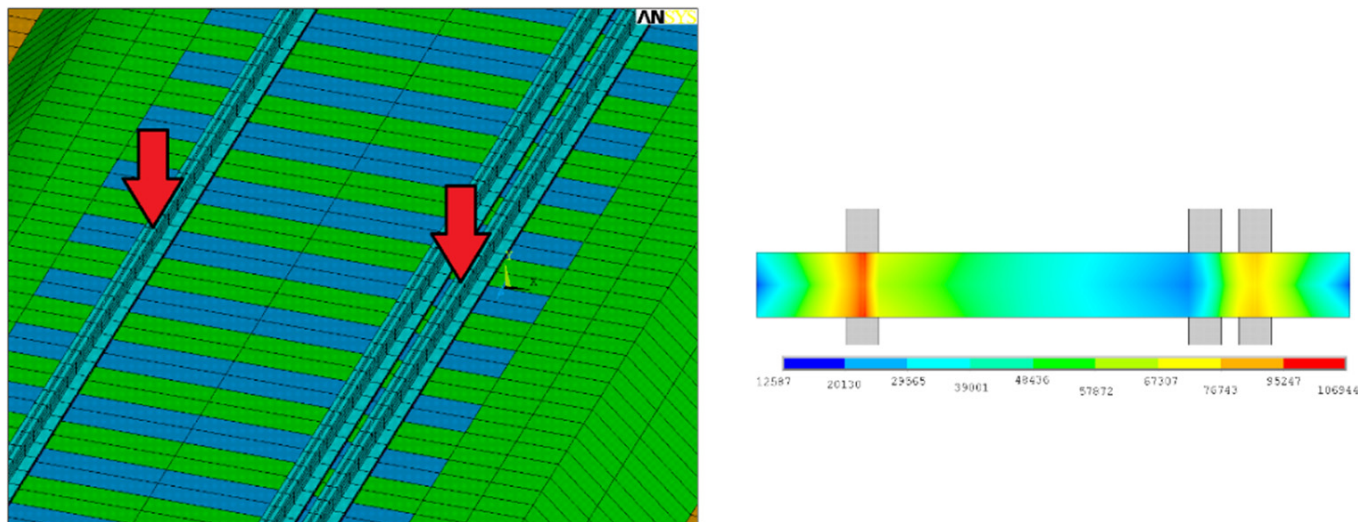
Fig. 12. Contact force distribution on sleeper-ballast interface, Civia train.

imum amplitude at a frequency of 800 Hz. It also presents another clear peak at 1400 Hz.

In addition, Fig. 10 shows the comparison between experimental and numerical rail accelerations at the sleeper for the passage of the commuter train running at speed of 80 km/h on Iberian gauge. In this case, the model achieves an rMSE of 24.9% for the common rail, and and rMSE of 24.6% for the outer rail. Again, significant differences between both rails were observed. In the time domain, peaks in the outer rail are 50–100% higher than in the common rail. In terms of frequency, in both cases, three main frequency intervals may be observed: 0–200, 400–600 and 900–1100 Hz. Nevertheless, the outer rail shows more relevant amplitudes in the frequency interval between 600 and 900 Hz, as well as two clear peaks at 1200 Hz and 1300 Hz.

Since the track under study is regularly maintained and support conditions remain constant along the entire sleeper, the track stiffness should be generally uniform along the track section. However, in the case of dual gauge track, vertical rail accelerations show a significant difference when compared to the other side. This is due to the uneven mechanic behaviour introduced by the loss of symmetry along the track axis. It can therefore be asserted that differences come mainly from the presence of the third rail, which increase the steel section and, consequently, the stiffness of the track. In fact, the vertical rail accelerations are significantly higher in the side with two rails, because both rails are fixed on the sleeper, strengthening the track only on one side. This effect might increase track degradation, as well as rail wear, fatigue, track settlement, and so on.

4.2. Sleeper-ballast stress analysis

Because of its newness, the measurement of the sleeper pressures in dual gauge tracks has not been previously reported in the literature. In addition, it was not possible to install load cells in the test site, so the stresses on the dual gauge track transmitted to the ballast layer were exclusively analysed using the numerical model described previously. It should be noted that ballast is modelled as a continuum material, while the sleeper-ballast interface was simulated by means of contact elements to ensure interaction and load transfers among the components [20,20]. Under these conditions, the friction can be estimated using geotechnical criteria assuming perfect interaction between concrete and granular materials. This is assumed as 45 of the friction angle of the ballast.

Once the vertical applied load on the top head of each rail are determined, the contact pressure can be calculated for trains running on standard or Iberian gauge. As can be seen in Fig. 11, the contact pressure is distributed evenly throughout the concrete sleeper with some concentrated values in small areas located under the rail seats. Moreover, it is observed that contact pressure has higher values at the inner rail than at the common rail. It is observed from the numerical analysis that, at a 100 kN rail seat load, the maximum sleeper-ballast pressure increases by 35% from 90 KPa to nearly 121 KPa when comparing the pressures obtained beneath the rail seats.

On the other hand, when considering commuter trains running on Iberian gauge, the region that experiences the highest magnitude of sleeper-ballast pressure is the area under the common rail, as shown in Fig. 12. Particularly, the contact force in the common rail is approximately 50% higher than that in the outer rail.

Considering that the proposed model assumes a uniform support below the level of the sleeper, the above-mentioned differences could be associated with the geometrical conditions and the gauge on which each train is running. This effect is most probably caused by structural changes in the rail-sleeper system, which governs stress transfer from the wheel-rail interface into the ballast layer. Although one rail is not loaded, the three rails must together simultaneously support loads because they are all fixed by clips.

5. Conclusions

With the implementation of an interoperable dual gauge railway tracks in Spain, there is a need to develop new studies to understand the mechanical phenomena occurring on the rail-sleeper grid of the track. Up to date, the response and behaviour of dual gauge tracks are unclear, especially those under dynamic conditions. Thus, this paper investigates the dynamic behaviour of dual gauge tracks using experimental and numerical simulations on a straight section. The results are summarized below.

1. Based on the measured data, characteristics of vertical rail and sleeper vibration accelerations are obtained experimentally for the first time. It is observed that the maximum vertical rail

I. Villalba Sanchis, R. Insa Franco, P. Martínez Fernández et al.

Construction and Building Materials 299 (2021) 123943

accelerations are significantly higher on the side with two adjacent outer rails. This effect is most probably caused by structural changes due to the presence of the third rail, which increases the steel section, especially on one side of the track.

2. To assess quantitatively the behaviour of dual gauge track, a numerical finite element model has been developed by use of the FEA software package. Comparisons between the results of the experimental and numerical model showed a good agreement in terms of vertical accelerations. In fact, it is possible to notice that the amplitudes of the vibrations calculated at various points are quite close to the experimental values.

3. To extend the analysis, the numerical model was employed to understand how the stresses are transmitted to the ballast layer. For the case investigated, results showed that contact pressure at the sleeper-ballast interface is highly variable on the bottom surface of the sleeper. Particularly, loads on the narrower rails generates maximum contact pressures under the inner rail, while loads on the wider gauge rails tend to be concentrated under the common rail.

4. -All things considered, the numerical and experimental results demonstrate the asymmetric nature of the dual gauge track behaviour. Consequently, differential track structure response caused by train forces can lead to significant economic loss for track owners through damage to rails, sleepers and ballast layer. To minimize this effect, softer rail pads and implementation of under sleeper pads may mitigate the risk of differential track settlement by lowering the sleeper–ballast contact pressure, although further analysis is required to ensure this.

These conclusions represent a first assessment of the dynamic behaviour of dual gauge tracks, which highlight the inherent asymmetry of such tracks and how they react quite differently depending on whether the train passing through uses the narrower or wider track gauge. However, there is still uncertainties as to why these differences happen and what long-term effects may have on the degradation and maintenance needs of the track. Consequently, data should be gathered repeatedly over a long period of time to characterise the wear and tear of the infrastructure. Additionally, further FEM modelling could be done to study in more detail the contact forces between sleepers and ballast and how these may affect ballast degradation. Finally, mitigation measures to address the detected asymmetrical behaviour (such as using softer rail pads, as proposed in conclusion number four) should be modelled and studied.

CRediT authorship contribution statement

Ignacio Villalba Sanchis: Conceptualization, Methodology, Software, Formal analysis, Data curation, Writing - original draft, Writing - review & editing. **Ricardo Insa Franco:** Conceptualization, Supervision. **Pablo Martínez Fernández:** Formal analysis, Investigation. **Pablo Salvador Zuriaga:** Data curation, Formal analysis, Validation.

Declaration of Competing Interest

The authors declare that they have no known competing financial interests or personal relationships that could have appeared to influence the work reported in this paper.

References

[1] H. Takemiya, Simulation of track−ground vibrations due to a high-speed train: the case of X-2000 at Ledsgard, J. Sound Vib. 261 (3) (2003) 503–526, https://doi.org/10.1016/S0022-460X(02)01007-6.

[2] E. Celebi, Three-dimensional modelling of train-track and sub-soil analysis for surface vibrations due to moving loads, Appl. Math. Comput. 179 (I) (2006) 209–230, https://doi.org/10.1016/j.amc.2005.11.095.

[3] D. Connolly, A. Giannopoulos, M.C. Forde, Numerical modelling of ground borne vibrations from high-speed rail lines on embankments, Soil Dyn. Earthq. Eng. 46 (2013) 13–19, https://doi.org/10.1016/j.soildyn.2012.12.003.

[4] P. Martínez Fernández, I. Villalba Sanchís, F. Botello Rojas, R. Insa Franco, Monitoring and analysis of vibration transmission for various track typologies. A case study, Transp. Res. D Transp. Environ. 24 (2013) 98–109, https://doi.org/10.1016/j.trd.2013.05.003.

[5] S. François, G. Lombaert, G. Degrande, Local and global shape functions in a boundary element formulation for the calculation of traffic induced vibrations, Soil Dyn. Earthq. Eng. 25 (2005) 839–856, https://doi.org/10.1016/j.soildyn.2005.05.002.

[6] P. Galvín, A. Romero, J. Domínguez, Fully three-dimensional analysis of high speed train/track/soil−structure dynamic interaction, J. Sound Vib. 329 (24) (2010) 5147–5163, https://doi.org/10.1016/J.JSV.2010.06.016.

[7] P.A. Costa, R. Calçada, A.S. Cardoso, Influence of train dynamic modelling strategy on the prediction of track−ground vibrations induced by railway traffic. Proc Inst Mech Eng, Part F: J Rail Rapid Transit, 226 (4) (2012), pp. 434-450, 10.1177%2F0954409711433686.

[8] A. Yaseri, M.H. Bazyar, N. Hataf, 3D coupled scaled boundary finite element/ finite-element analysis of ground vibrations induced by underground train movement, Comput. Geotech. 60 (2014) 1–8, https://doi.org/10.1016/j.compgeo.2014.03.013.

[9] N. Correia dos Santos, J. Barbosa, R. Calçada, R. Delgado, Track-ground vibrations induced by railway traffic: experimental validation of a 3D numerical model, Soil Dyn. Earthq. Eng 97 (2017) 324–344, https://doi.org/10.1016/j.soildyn.2017.03.004.

[10] G. Kouroussis, O. Verlinden, Prediction of railway induced ground vibration through multibody and finite element modelling, Mech. Sci. 4 (2017), https://doi.org/10.5194/MS-4-167-2013.

[11] Renfe, Our trains. https://www.renfe.com/es/en/renfe-group/renfe-group/fleet-of-trains.

[12] E. Fortunato, R. Resende, Mechanical behaviour of railway track structure and foundation – three-dimensional numerical modelling. Railway Foundations (RailFound'06), Birmingham, UK (2006), pp. 217-227.

[13] M. Banimahd, P. Woodward, J. Kennedy, G. Medero, Three-dimensional modelling of high speed ballasted railway tracks. Proc Inst Mech Eng – Transport, 166 (2) (2013), pp. 113-123. doi: 10.1680/tran.9.00048.

[14] D. Ribeiro, R. Calçada, R. Delgado, M. Brehm, V. Zabel, Finite-element model calibration of a railway vehicle based on experimental modal parameters, Veh. Sys. Dyn. 51 (6) (2013) 821–856, https://doi.org/10.1080/00423114.2013.778416.

[15] X. Li, M. Ekh, J.C.O. Nielsen, Three-dimensional modelling of differential railway track settlement using a cycle domain constitutive model, Int. J. Numer. Anal. Meth. Geomech. 40 (12) (2016) 1758–1770, https://doi.org/10.1002/nag.2515.

[16] J.C.O. Nielsen, X. Li, Railway track geometry degradation due to differential settlement of ballast/subgrade – numerical prediction by an iterative procedure, J. Sound Vib. 412 (2018) 441–456, https://doi.org/10.1016/j.jsv.2017.10.005.

[17] J.N. Varandas, A. Paixão, E. Fortunato, B. Zuada Coelho, P. Hölscher, Long-term deformation of railway tracks considering train-track interaction and non-linear resilient behaviour of aggregates – a 3D FEM implementation, Comput. Geotech. 126 (2020), https://doi.org/10.1016/j.compgeo.2020.103712 103712.

[18] D.G. de Infraestructuras ferroviarias. Centro de Publicaciones. M° de Fomento. Recomendaciones para el proyecto de plataformas ferroviarias, 1999.

[19] E. Chaves, Notes on continuum mechanics, Sprinter/CIMNE, 2012, Spain.

[20] I. Gallego, J. Muñoz, S. Sanchez-Cambronero, A. Rivas, Recommendations for numerical rail substructure modeling considering nonlinear elastic behavior, J. Traffic Transp. Eng. 139 (8) (2013) 848–858, https://doi.org/10.1061/(ASCE)TE.1943-5436.0000560.

[21] J. Molines, J. Medina, Explicit wave-overtopping formula for mound breakwaters with crown walls using CLASH neural network-derived data, J. Waterway Port Coastal Ocean Eng. 142 (3) (2016) 04015024, https://doi.org/10.1061/(ASCE)WW.1943-5460.0000322.

Further reading

[22] X. Sheng, C.J.C. Jones, D.J. Thompson, Response of infinite periodic structures to moving or stationary harmonic loads, J. Sound Vib. 282 (2005) 125–149, https://doi.org/10.1016/j.jsv.2004.02.050.